ECHANOSYNTHESIS AND MAGNETIC PROPERTIES OF NANOCRYSTALLINE $LaFeO_3$ USING DIFFERENT IRON OXIDES

A.A. Cristóbal [1], P.M. Botta [1], P.G. Bercoff [2], J.M. Porto López [1]

[1] Instituto de Investigaciones en Ciencia y Tecnología de Materiales, INTEMA (CONICET-UNMdP), J.B Justo 4302 (B7608FDQ) Mar del Plata, Argentina.

[2] Facultad de Matemática, Astronomía y Física, FaMAF (UNC), Ciudad Universitaria (5000) Córdoba, Argentina. CONICET.

ABSTRACT

The synthesis of the orthoferrite $LaFeO_3$ using high-energy ball-milling of La_2O_3 and Fe_3O_4 or α-Fe_2O_3 oxides and subsequent thermal treatments of resulting powders was studied. The phase evolution during the mechanical treatment was analyzed by X-ray diffraction (XRD), differential thermal analysis (DTA) and scanning electron microscopy (SEM). Also, magnetic properties of the obtained materials were measured at room temperature by vibrating sample magnetometry (VSM). From 30 minutes of mechanochemical activation the gradual disappearance of reactants and the formation of $LaFeO_3$ were observed. For both reactive mixtures the reaction was completed after 3 h of milling. Magnetic hysteresis loops of these mechanoactivated samples showed a significant ferromagnetic component in $LaFeO_3$. This behavior was interpreted on the basis of a spin-canting effect induced by the mechanochemical treatment. Thermal treatments allowed the relaxation of the distorted structure, resulting in the formation of the conventional antiferromagnetic $LaFeO_3$ phase.

KEYWORDS: A. oxides, A. magnetic materials, D. magnetic properties.

INTRODUCTION

Perovskite oxides ABO_3 (where A is a rare-earth element and B is a 3d transition metal) have attracted considerable attention because of their wide applications, such as fuel cells, catalysis and gas sensors [1-5]. $AFeO_3$ oxides (the so-called orthoferrites) belong to a relevant class of weak ferromagnetic materials with interesting magnetic and magneto-optical properties [6-7]. The magnetic structure in orthoferrites can be conventionally described by two interpenetrating pseudo-cubic face centred sub-lattices in which each Fe^{3+} ion is surrounded by six O^{2-} ions. This results in a collinear arrangement of the two sub-lattices, giving an antiferromagnetic ordering. However, the FeO_6 octahedra can be tilted to different degrees depending on the size of the rare earth cation, leading to a net magnetic moment [8-9].

Nanocrystalline $LaFeO_3$ is required for several applications and it has been prepared by different methods including coprecipitation, sol-gel, hydrothermal processes, and other preparative routes [10-14]. Zhang et al. [15] have employed a mechanochemical method to obtain nanocrystals of $LaFeO_3$ at room temperature using La_2O_3 and Fe_2O_3 as reactants. However, the effect of this synthesis method on the magnetic behavior of the resulting material was not studied. Mechanochemical activation has been used during the last decades as a powerful tool for the preparation of metastable crystalline and amorphous phases, and nanostructured materials not-obtainable through conventional methods [16-18]. This is due to three fundamental reasons: shortening of reaction times, reduction of the high temperatures usually required for developing solid state reactions and the possibility of obtaining materials with special properties. The high concentration of lattice defects introduced by the mechanical treatment often produces phases with distorted crystalline structures, far from the thermodynamic equilibrium. For this reason several transition metal oxides (ferrimagnetic spinels, ferro and

piezoelectric perovskites, etc) with modified cation distributions could be obtained using this relatively simple methodology [19-22].

In this work, a room-temperature mechanochemical method is proposed to prepare nanocrystalline $LaFeO_3$. The effects of the synthesis route and the nature of the employed iron oxides on the physicochemical and magnetic properties of the obtained material are analyzed.

EXPERIMENTAL

Preparation of samples

Starting materials were La_2O_3 (commercial reagent, 99.99 wt %, particle size lower than 1 μm), and iron oxides, magnetite (Fe_3O_4) and hematite (α-Fe_2O_3). Magnetite was a concentrate of magnetite ore (≥ 97.5 wt% Fe_3O_4, particle size lower than 44 μm) from Sierra Grande (Chubut, Argentina), and hematite was a commercial reagent (≥ 97 wt%, particle size lower than 1 μm). The major impurities in magnetite were a clay mineral (illite), and quartz (both in similar concentrations). Hematite contains mainly amorphous silica and quartz. Highly hygroscopic La_2O_3 was calcined for 2 h at 1000ºC before being used. After heating, the oxide was cooled down to room temperature in a desiccator, and then immediately used to prepare the samples. With these oxides two series of samples were prepared. In the so-called series ML a mixture of La_2O_3:Fe_3O_4 in a molar ratio of 2:3 was mechanically activated. The other series (named HL) was obtained by mixing La_2O_3 and hematite in a molar ratio of 1:1.

A planetary laboratory ball-mill (Fritsch Pulverisette 7) with vials and balls of hardened Cr-steel was used for the mechanochemical treatment of both powder mixtures. The samples were activated under air atmosphere. The milling bowls were loaded with 5 g of powder mixture and 7 balls of 15 mm diameter each, resulting in a ball-to-powder

mass ratio of 20:1, and rotated at 1500 rpm during different times. The obtained samples were labeled MLxh and HLxh, where x is the activation time in hours.

Samples activated for 3 h were thermally treated during 30 min under air atmosphere at temperatures ranging from 600 to 1000ºC. These milled and calcined powders were called MLxh-*y* and HLxh-*y*, being *y* the temperature of the thermal treatment.

Characterization and magnetic properties

The crystalline phases were characterized by X-ray diffraction (XRD) using a Philips goniometer coupled to a PW 1830/40 power generator, using CoKα radiation (λ = 1.78897 Å) at 40 kV and 30 mA, with an iron filter. All the diffractograms were scanned between 10° and 80° 2θ with a step size of 0.01°.

The microstructure and elemental composition of both starting mixtures and the activated samples were examined in a scanning electron microscope (SEM, Philips 505). Electron probe microanalyses (EPMA) were carried out with an EDAX analyzer attached to the microscope. Prior to the observations, the samples were coated with gold.

Differential thermal analyses (DTA) were performed in a Shimadzu DTA-50H equipment under flowing synthetic air, using a heating rate of 10ºC/min and samples of approximately 40 mg.

All the samples were magnetically characterized at room temperature in a vibrating sample magnetometer (VSM) LakeShore 7300 coupled to an electromagnet which is able to produce a magnetic field up to 15 kOe. For each sample, maximum magnetization (M_{max}) and coercivity (Hc) were obtained from the corresponding hysteresis loop. M_{max} is the magnetization measured at the highest applied field, i.e., 15

kOe. Saturation magnetization *(Ms)* was estimated in each case from a linear extrapolation of M vs H^{-1} curves at high field values.

RESULTS AND DISCUSSION

Figures 1a and 1b show the evolution of XRD patterns of samples ML and HL, respectively, with the activation time. In both cases it is possible to observe how the diffraction peaks corresponding to $LaFeO_3$ arise. The appearance of orthoferrite peaks can be observed for milling times as short as 30 min. However, the peaks corresponding to the reactants do not completely disappear until 2 h of activation. After 3 h of milling the only detectable crystalline phase both in samples ML and HL is $LaFeO_3$.

As the milling progresses, the intensity of the orthoferrite diffracted peaks increases and their line-width broadens. Crystallite sizes were determined by FWHM measurements and using the Scherrer equation [23]. These are approximately 15 nm for the activated samples and increase significantly after thermal treatments at 1000ºC up to ~ 60 nm (Table 1). This is an expected effect because of the deterioration of the crystalline structure of $LaFeO_3$ by mechanochemical treatment and its subsequent recrystallization produced by thermal treatment.

Figures 2a and 2b show the XRD patterns of samples ML3h and HL3h after heating at 600, 800 and 1000ºC. As temperature increases a continuous refinement of the orthoferrite crystalline structure can be observed. It could be expected that during the heating, the structural defects accumulated by the activation would be healed. XRD diagrams of ML3h-1000 and HL3h-1000 reveal the presence of well-crystallized $LaFeO_3$ as the only component of these powders.

Figures 3a and 3b display DTA scans for series ML and HL, respectively. At 365 and 527ºC two endothermic peaks are clearly observed for ML0h and HL0h. These thermal events correspond to dehydration of $La(OH)_3$, which was formed after weighting the

reactants for the preparation of powder mixtures. During the milling these endothermic peaks disappear for longer activation times, revealing the gradual consumption of the reactants together with the formation of $LaFeO_3$.

A wide exothermic band is observed at temperatures ranging from 200 to 300ºC for ML1h and ML2h. A decrease of intensity and a shift to lower temperatures as the activation progresses can be noticed. All these observations lead us to assign this thermal event to the oxidation of magnetite that remains from the mechanical activation, as previously reported for a similar reactive mixture [24]. The absence of exothermic bands in series HL supports this assertion.

Scanning electron micrographs (Figure 4) of activated powders show the loss of the original morphology of the reactants' particles (especially for samples ML). ML1h and HL1h are composed of agglomerates of irregular-shaped particles, which have a mean size below one micron. EPMA results (not shown in this paper) indicate a homogeneous distribution of Fe and La in the entire samples, at least in the volume range analyzed by the microprobe (1 μm^3).

Magnetic hysteresis loops for both series of activated samples are shown in Figure 5. The resulting *M*s and *H*c values for each sample are summarized in Table 1. For series ML a monotonic decrease of saturation magnetization with milling time is observed, reaching values as low as 1.6 emu/g for ML3h. Coercivity shows a substantial increase after the first 30 min of activation, but from 1h on it progressively diminishes. The magnetic behavior of series ML is consistent with the reaction occurring inside the mill. The consumption of ferrimagnetic magnetite and the simultaneous appearance of antiferromagnetic $LaFeO_3$ produce a marked fall of *M*s. The increment of *H*c in the first stages of the activation can be explained by the reduction of domain size in magnetite, which is still the main phase in ML0.5h, according to XRD results (Fig. 1a). After 2h of

activation the formation of $LaFeO_3$ is already very advanced, producing an expected decrease in *H*c.

The magnetic behavior of series HL presents some differences with respect to samples ML's. The hysteresis loop for the non-activated sample reveals the typical response of hematite, which is a canted antiferromagnet at room temperature, above the Morin transition [25]. A decrease of *M*s after the first 30 min of activation is observed, followed by a continuous increase for longer activation times. This behavior is opposite to that exhibited by series ML, where the mechanical treatment produces a drop of *M*s as a consequence of the progressive formation of $LaFeO_3$ at the expense of the ferrimagnetic phase, Fe_3O_4. For series HL the main effect of the milling is also the formation of orthoferrite (see Fig. 1b), but in this case the product has a higher *M*s than its parent iron phase (hematite). This fact would indicate that the mechanosynthesized $LaFeO_3$ behaves as a weak ferromagnet. This is a quite interesting result because the expected values of *M*s for antiferromagnetic $LaFeO_3$ are lower than that obtained for the completely reacted sample HL3h. The similarity between the values of *M*s and *H*c corresponding to ML3h and HL3h (see Table 1) indicates that in spite of being obtained from different iron oxides both perovskite phases have the same distorted antiferromagnetic structure. As stated earlier, the crystalline structure of orthoferrites can be considerably deformed from the ideal perovskite structure and the FeO_6 octahedra can be significantly tilted. This could result in a non-collinear arrangement of the two magnetic sub-lattices producing a residual moment. In this way the main effect of the mechanochemical treatment is probably to provoke a significant distortion in the crystal structure of $LaFeO_3$ leading to a non-negligible net magnetic moment. It is worth remarking that the magnetic moment obtained here for $LaFeO_3$ is even higher

than those reported previously for nanocrystalline samples [26] synthesized by other method.

Figures 6a and 6b show the hysteresis loops *M* vs *H* for samples ML3h and HL3h calcined at several temperatures. Similar results were obtained for both series. As temperature increases a monotonic drop of *M*s is noticed, revealing an evolution of the distorted magnetic structure of $LaFeO_3$ towards an antiferromagnetic ordering. Curves registered for samples heated at 1000ºC exhibit different responses (see insets of Figs. 6a and 6b). HL3h-1000 presents a linear dependence of *M* with *H* and absence of hysteresis, indicating the existence of a complete antiferromagnetic ordering in the perovskite phase. This tendency to the collinear arrangement of magnetic moments at higher temperatures is also observed for ML3h-1000. However, in this case a weak ferromagnetic behavior still remains, suggesting an influence of the nature of the iron oxide used in the synthesis on the magnetic structure of $LaFeO_3$.

CONCLUSIONS

The mechanochemical activation of La_2O_3 and Fe_3O_4 or α-Fe_2O_3 allowed the synthesis of nanocrystalline $LaFeO_3$ in very short reaction times and using a much simpler preparative technique than the usual solid-state reaction and wet-chemistry methods.

The mechanosynthesized $LaFeO_3$ behaves as a weak ferromagnet with a relatively high saturation magnetization in comparison with previously reported results. This interesting magnetic response suggests that mechanochemical activation induced a distortion in the perovskite crystalline structure, which provoked significant spin-canting.

Thermal treatments produced the healing of the structural defects accumulated during the mechanochemical activation leading to an antiferromagnetic ordering of the distorted $LaFeO_3$ structure.

REFERENCES

[1] L.W.Tai, M.M. Natallah, H.U. Anderson, D.M. Sparlin, S.R.Schin. Solid State Ionics 76 (1995) 273-283.

[2] N.Q. Minh, J. Am. Ceram. Soc. 76 (1993) 563–568.

[3] J.G. McCarty, H. Wise, Catal. Today 8 (1990) 231-248.

[4] E. Traversa, S. Matsushima, G. Okada, Y. Sadaoka, Y. Sakai, K. Watanabe, Sens. Actuators B 25 (1995) 661-664.

[5] E. Traversa, S. Villanti, G. Gusmano, H. Aono, Y. Sadaoka, J. Am. Ceram. Soc. 82 (1999) 2442-2450.

[6] D. Treves, J. Appl. Phys. 36 (1965) 1033-1039.

[7] Y.S. Didosyan, H. Hauser, H. Wolfmayr, J. Nicolics, P. Fulmek, Sens. Actuators A 106 (2003) 168-171.

[8] S. Mathur, M. Veith, R. Rapalavicuite, H. Shen, G.F. Goya, W.L.M. Filho, T.S. Berquo, Chem. Mater. 16 (2004) 1906-1913.

[9] S. Mathur, H. Shen, N. Lecerf, A. Kjekshus, H. Fjellvag, G.F. Goya, Adv. Mater., 14 (2002) 1405-1409.

[10] X. Li, H.B. Zhang, M. Y.Zhao, Mater. Chem. Phys., 37 (1994) 132-135.

[11] C. Vázquez-Vázquez, P. Kogerler, M.A. López-Quintela, R.D. Sanchez, J. Rivas, J. Mater. Res. 13 (1998) 451-456.

[12] W. Zheng, R. Liu, D. Peng, G. Meng, Mater. Lett. 43 (2000) 19-22.

[13] C. Shivakumara. Solid State Comm. 139 (2006) 165-169.

[14] A.D. Jadhav, A.B. Gaikwad, V. Samuel, V. Ravi. Mater. Lett. 61 (2007) 2030-2032.

[15] Q. Zhang, F Saito, J. Mater. Sci. 36 (2001) 2287-2290.

[16] K. Tkácová, in: D.W. Fuerstenau (Ed.), Developments in Mineral Processing, vol. 11, Elsevier, Amsterdam, 1989.

[17] D.L. Zhang, Prog. Mater. Sci. 49 (2004) 537-560.

[18] C. Suryanarayana, E. Ivanov, V.V. Boldyrev, Mater. Sci. Eng. A 304–306 (2001) 151-158.

[19] B.H. Liu, J. Ding, Z.L. Dong, C.B. Boothroyd, J.H. Yin, J.B. Yi, Phys. Rev. B, 74, (2006) 184427.

[20] V. Šepelák, U. Steinike, D.Chr. Uecker, S. Wissmann, D. Becker, J. Solid State Chem. 135 (1998) 52-58.

[21] M. Algueró, J. Ricote, T. Hungría, A. Castro, Chem. Mater. 19 (2007) 4982-4990.

[22] P. M. Botta, P. G. Bercoff, E. F. Aglietti, H. R. Bertorello and J. M. Porto López, J. Mater. Sci., 37, (2002) 2563-2568.

[23] B.D Cullity. "Elements of X-Ray Diffraction", 2nd ed., Addison-Wesley Publ. Co., Reading, 1976.

[24] P.M. Botta, P.G. Bercoff, E.F. Aglietti, H.R. Bertorello, J.M. Porto López, Mater. Sci. Eng. A 360 (2003) 146-152.

[25] "Canted antiferromagnetism: hematite". A. H. Morrish. World Scientific, 1994. Chapter 4.

[26] M. Rajendran, A.K. Bhattacharya, J. Eur. Ceram. Soc. 26 (2006) 3675-3679.

FIGURE CAPTIONS

Figure 1. XRD patterns of samples ML (a) and HL (b) mechanically activated for several times.

Figure 2. XRD patterns of samples ML3h (a) and HL3h (b) thermally treated at selected temperatures.

Figure 3. Differential thermal analyses of the series of activated samples ML (a) and HL (b).

Figure 4. SEM micrographs of non-activated mixtures and samples activated for 1 h (ML1h and HL1h).

Figure 5. *M* vs *H* curves for the series of activated samples ML (a) and HL (b).

Figure 6. *M* vs *H* curves for samples ML3h (a) and HL3h (b) thermally treated at selected temperatures. The insets are enlargements showing the behavior of samples ML3h-1000 (a) and HL3h-1000 (b).

Table 1. Saturation magnetization (Ms), maximum magnetization (M_{max}) (measured at 15 kOe), coercivity (Hc) and crystallite size (d) of $LaFeO_3$ for series ML and HL.

Sample	Ms (emu/g)	M_{max} (emu/g)	Hc (Oe)	d (nm)
ML0h	40.7	39.8	65	--
ML0.5h	23.2	21.8	512	--
ML1h	11.9	11.1	500	16
ML2h	3.2	2.9	280	14
ML3h	1.6	1.4	129	15
ML3h 1000	0.2	0.1	151	59
HL0h	0.5	0.5	220	--
HL0.5h	0.4	0.3	210	--
HL1h	0.8	0.7	155	17
HL2h	1.2	1.0	108	15
HL3h	2.0	1.7	105	15
HL3h 1000	0.2	0.1	171	68

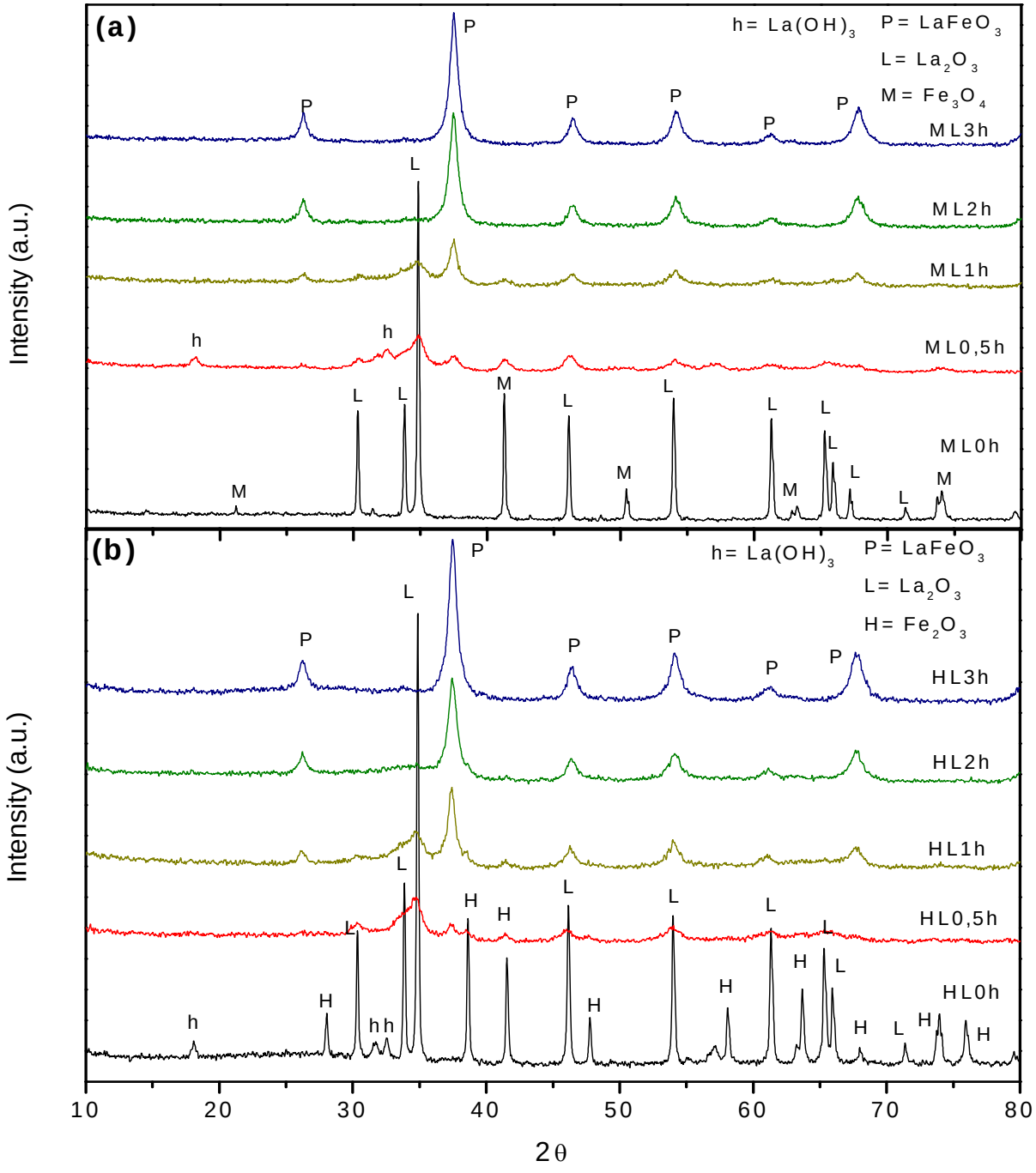
(a)
h= La(OH)3
P= LaFeO3
L= La2O3
M= Fe3O4
ML3h
ML2h
ML1h
ML0,5h
ML0h
(b)
h= La(OH)3
P= LaFeO3
L= La2O3
H= Fe2O3
HL3h
HL2h
HL1h
HL0,5h
HL0h
Intensity (a.u.)
Intensity (a.u.)
10
20
30
40
50
60
70
80
2θ

Figure 1

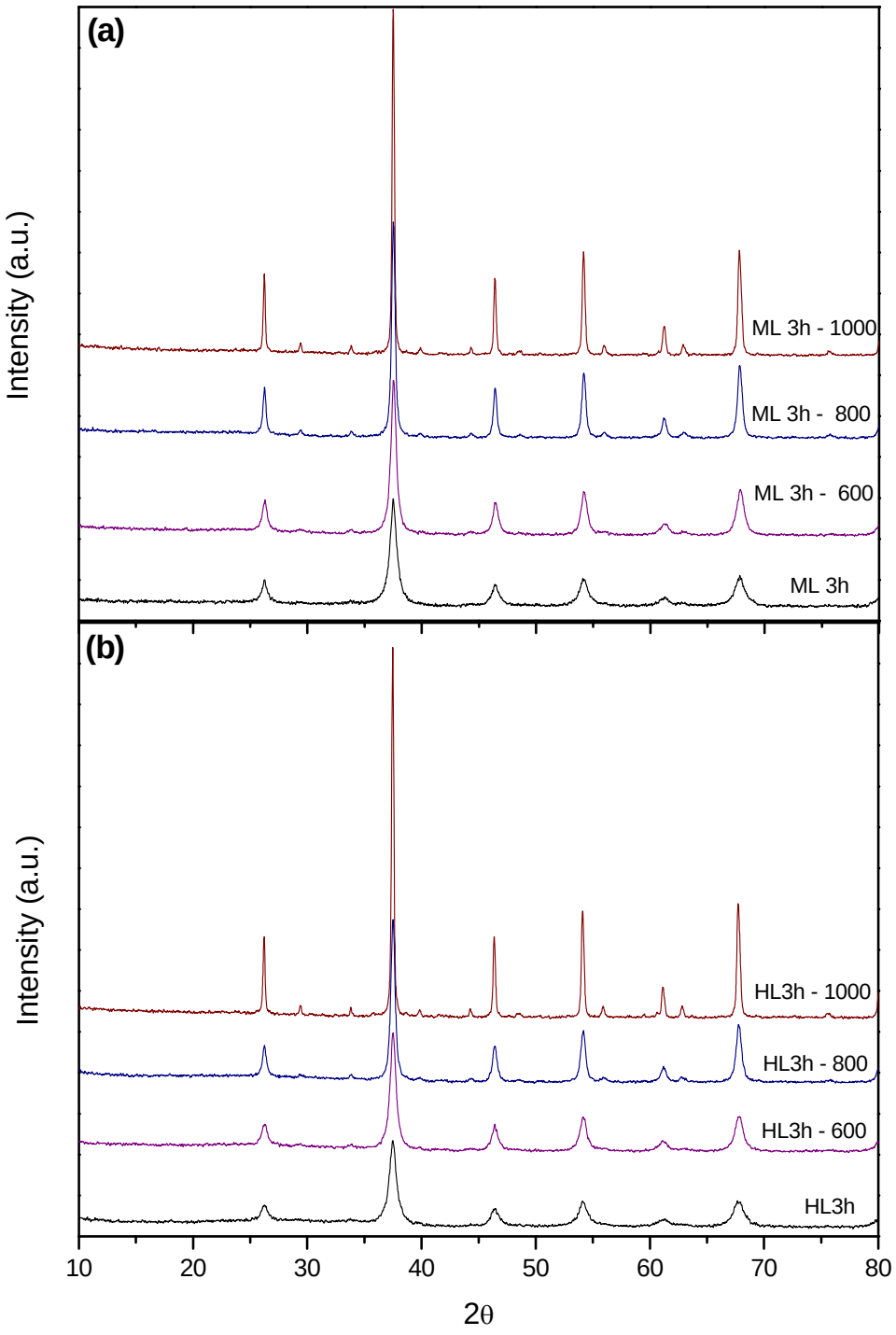
(a)
Intensity (a.u.)
ML 3h - 1000
ML 3h - 800
ML 3h - 600
ML 3h
(b)
Intensity (a.u.)
HL3h - 1000
HL3h - 800
HL3h - 600
HL3h
10
20
30
40
50
60
70
80
2θ

Figure 2

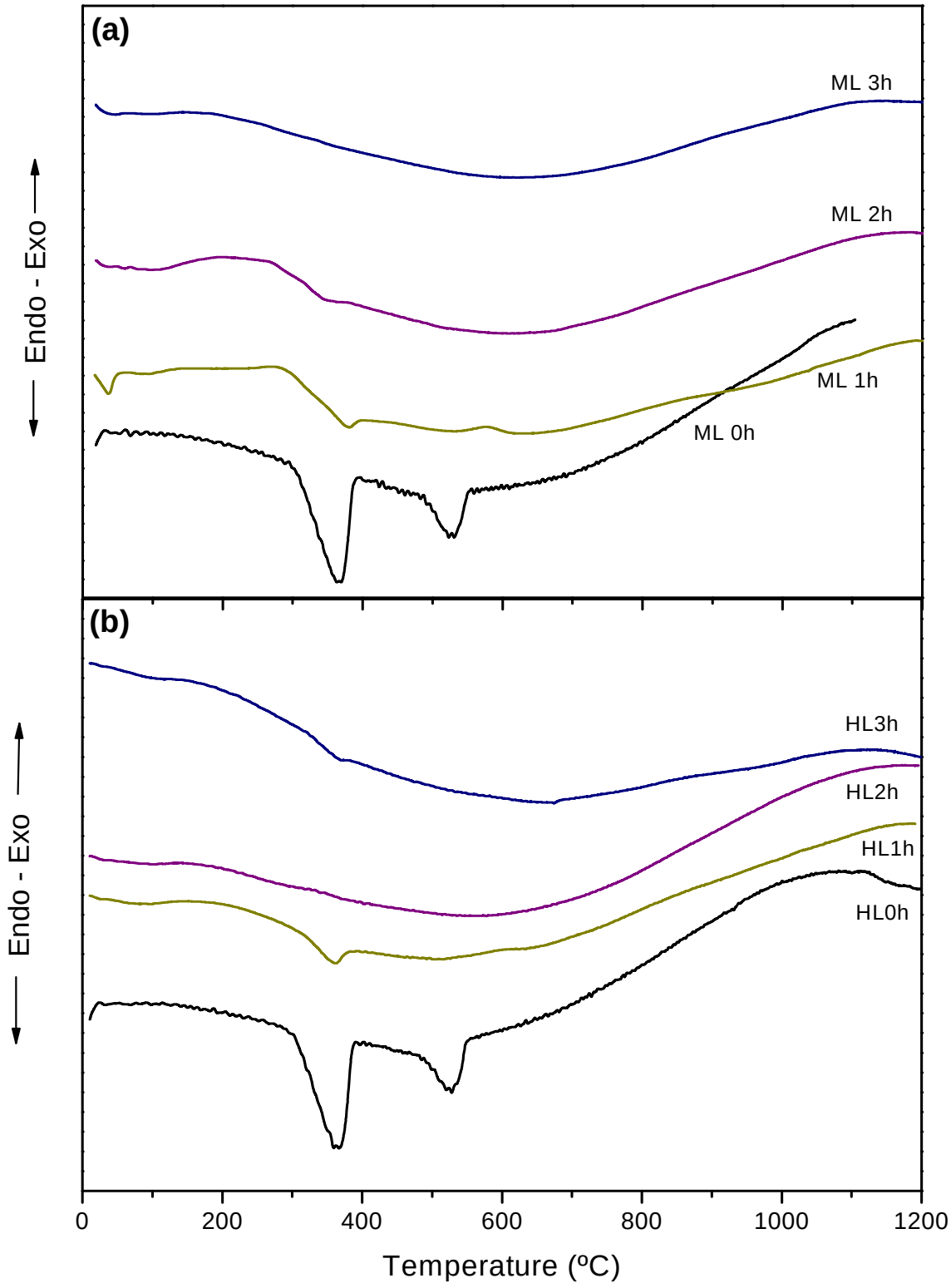
(a)
ML 3h
ML 2h
ML 1h
ML 0h
Endo - Exo
(b)
HL3h
HL2h
HL1h
HL0h
Endo - Exo
0
200
400
600
800
1000
1200
Temperature (ºC)

Figure 3

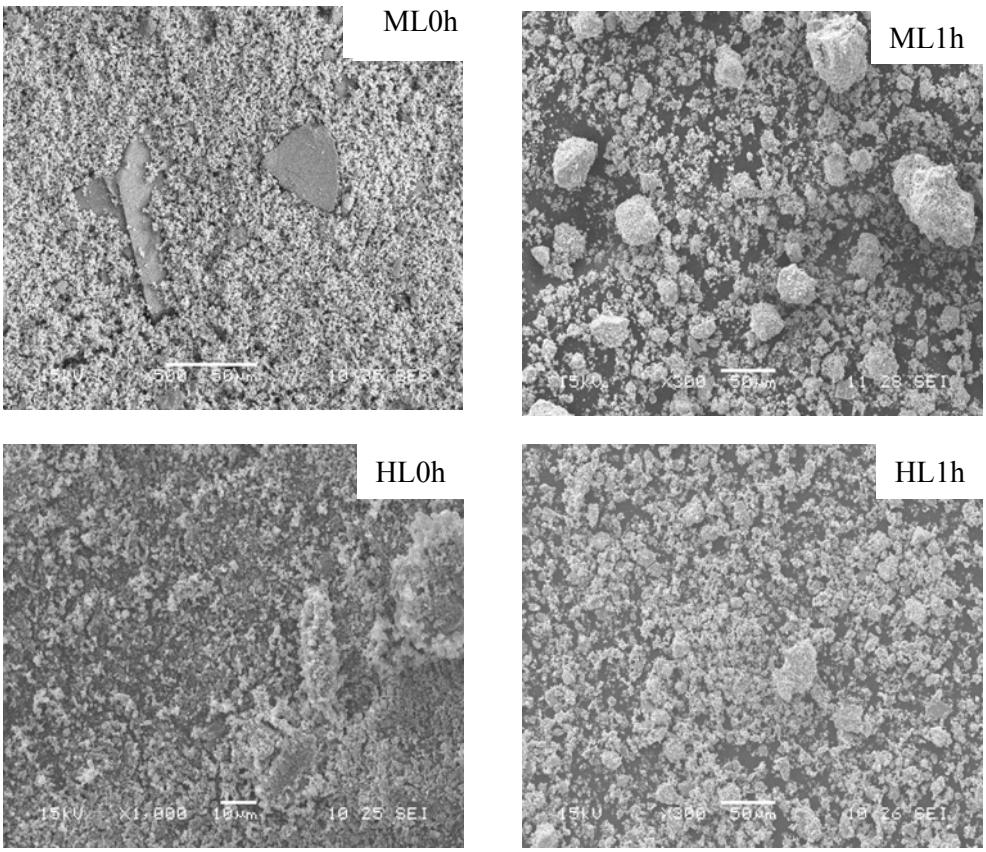

Figure 4

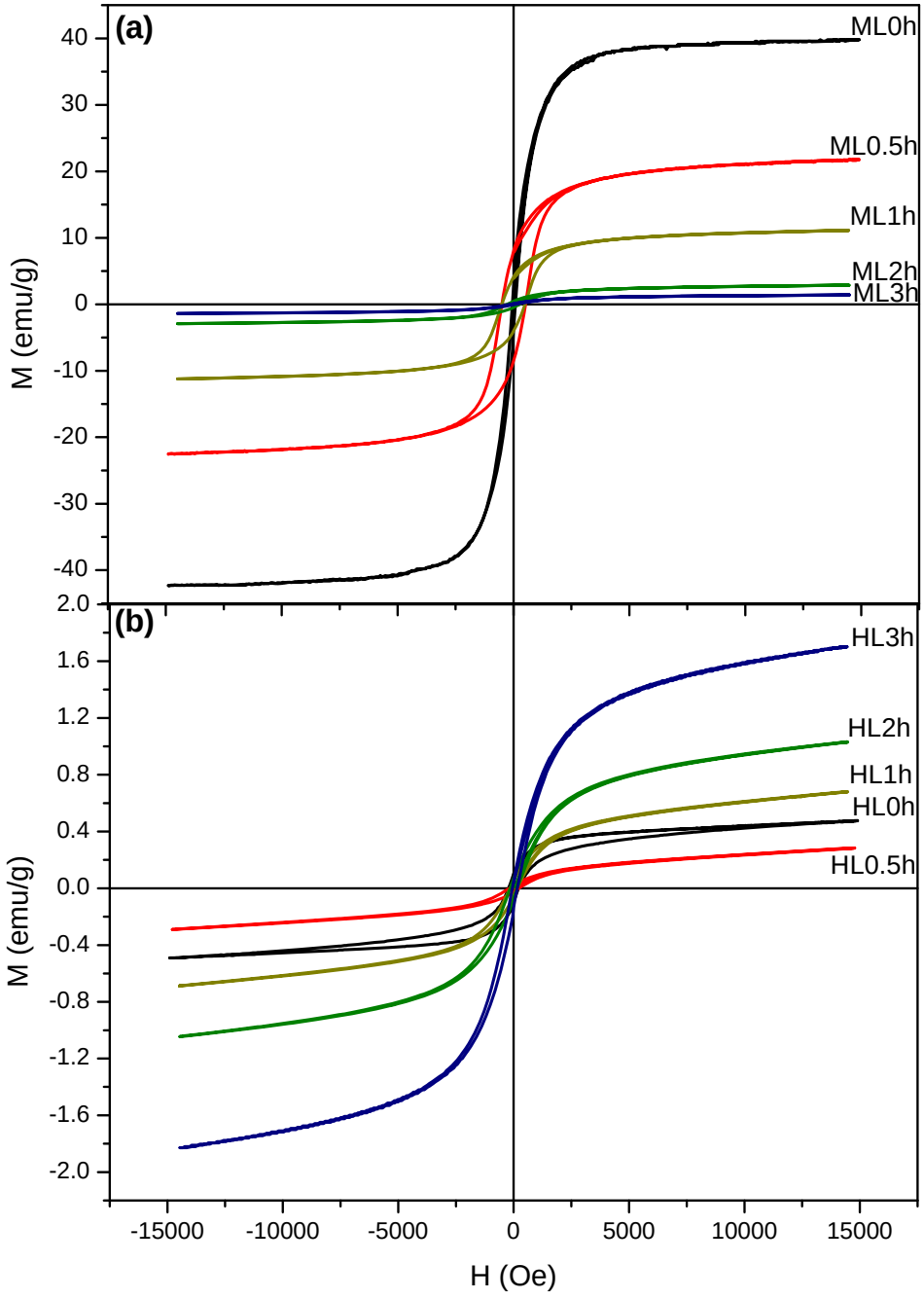
(a)
ML0h
ML0.5h
ML1h
ML2h
ML3h
M (emu/g)
40
30
20
10
0
-10
-20
-30
-40
(b)
HL3h
HL2h
HL1h
HL0h
HL0.5h
M (emu/g)
1.6
1.2
0.8
0.4
0.0
-0.4
-0.8
-1.2
-1.6
-2.0
-15000
-10000
-5000
0
5000
10000
15000
H (Oe)

Figure 5

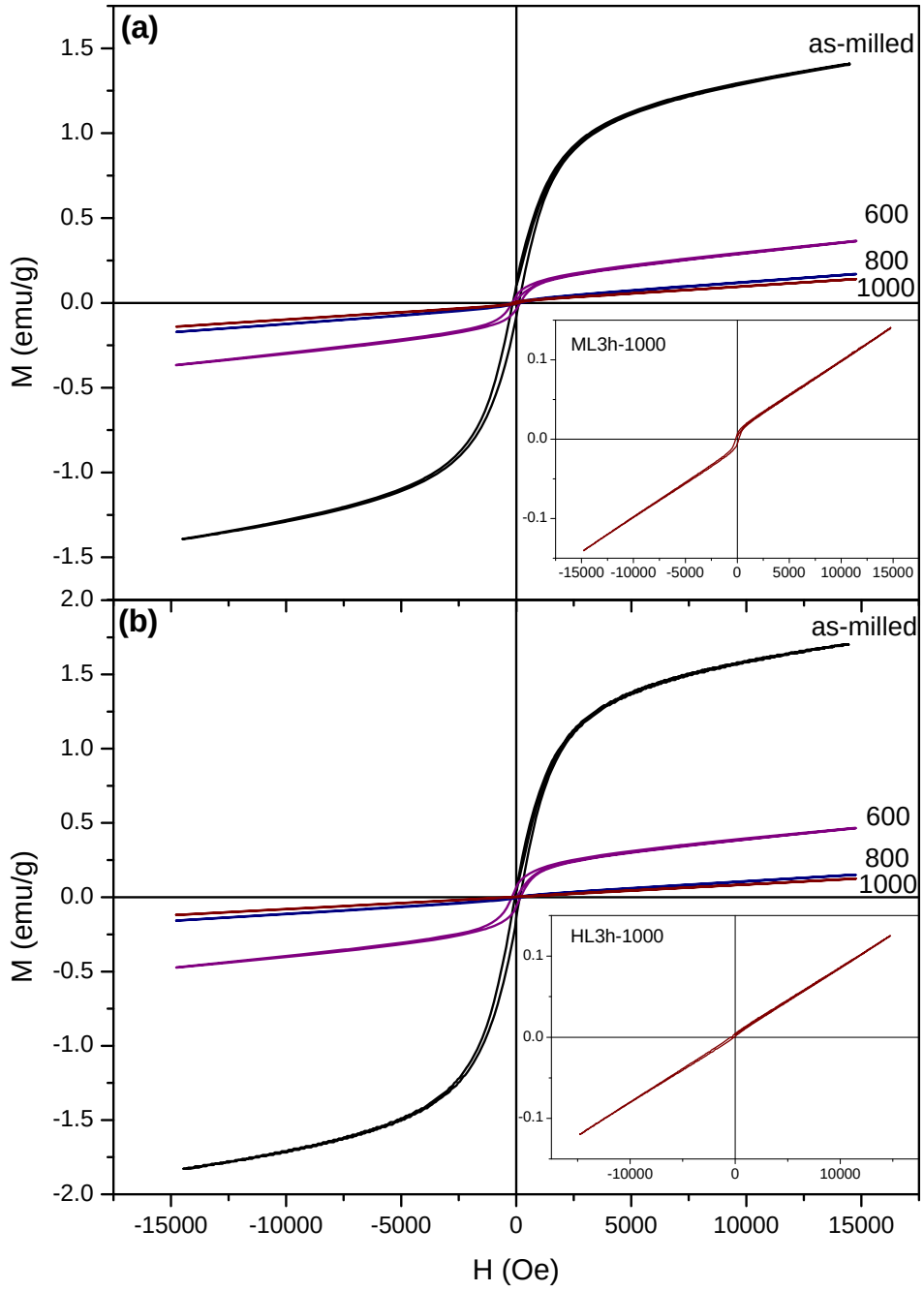
(a)
as-milled
600
800
1000
ML3h-1000
(b)
as-milled
600
800
1000
HL3h-1000
M (emu/g)
H (Oe)

Figure 6